

Article

Not peer-reviewed version

Spectral and Photometric Studies of NGC 4151 in the Optical Range: Current Results

[Nazim Huseynov](#) , [Saule Shomshekova](#) ^{*} , [Aleksander Serebryanskiy](#) , [Luydmila Kondratyeva](#) , Samira Rahimli , [Gabit Nazymbekov](#) , Inna Reva , [Gaukhar Aimanova](#)

Posted Date: 5 December 2025

doi: 10.20944/preprints202512.0355.v1

Keywords: active galaxies; Seyfert galaxies; NGC 4151; photometric variability; spectral variability; archival spectral data; supermassive black hole











Preprints.org is a free multidisciplinary platform providing preprint service that is dedicated to making early versions of research outputs permanently available and citable. Preprints posted at Preprints.org appear in Web of Science, Crossref, Google Scholar, Scilit, Europe PMC.

Copyright: This open access article is published under a [Creative Commons CC BY 4.0 license](#), which permit the free download, distribution, and reuse, provided that the author and preprint are cited in any reuse.

Disclaimer/Publisher's Note: The statements, opinions, and data contained in all publications are solely those of the individual author(s) and contributor(s) and not of MDPI and/or the editor(s). MDPI and/or the editor(s) disclaim responsibility for any injury to people or property resulting from any ideas, methods, instructions, or products referred to in the content.

Article

Spectral and Photometric Studies of NGC 4151 in the Optical Range: Current Results

Nazim Huseynov¹, Saule Shomshekova^{2,3,*}, Alexander Serebryanskiy²,
Luydmila Kondratyeva², Samira Rahimli¹, Gabit Nazymbekov², Inna Reva²
and Gaukhar Aimanova²

¹ Shamakhy Astrophysical Observatory named after N. Tusi, AZ-5626, Shamakhy district, Republic of Azerbaijan

² Fesenkov Astrophysical Institute, Observatory 23, Medeu District, 050020, Almaty, Kazakhstan

³ Abai Kazakh National Pedagogical University, Dostyk Ave. 13, 050010, Almaty, Republic of Kazakhstan

* Correspondence: shomshekova@fai.kz

Abstract

The present work reports the latest findings from photometric and spectroscopic studies of the Seyfert galaxy NGC 4151. Photometric and spectroscopic observations were carried out using the Zeiss-1000 and AZT-8 telescopes at the Tien Shan Astronomical Observatory (TSHAO) and the Kamenskoe Plateau Observatory of the Fesenkov Astrophysical Institute (FAI). In addition, photometric data were obtained at the Shamakhy Astrophysical Observatory (ShAO) with the "Zeiss 600" telescope in the Cassegrain focus. The collected data enabled us to construct light curves and perform a comparative analysis of both modern and archival spectral observations.

Keywords: active galaxies; Seyfert galaxies; NGC 4151; photometric variability; spectral variability; archival spectral data; supermassive black hole

1. Introduction

The study of spectral and photometric variability is an effective diagnostic tool for investigating the physical processes occurring in accreting compact supermassive objects, which constitute the majority of galaxies with active nuclei [1]. The characteristic timescales of this variability indicate the relatively compact sizes of the regions that emit the optical continuum and broad emission lines [2,3]. Investigating the spectral and photometric variability of galaxies is essential for understanding the structure and evolution of active galactic nuclei (AGN); without this knowledge, it is impossible to approach the problem of identifying the nature of the central energy source. Information on the properties of spectral and photometric variability in AGN must be taken into account to refine their theoretical models. Within the framework of the supermassive black hole model with an accretion disk, both periodic and stochastic variations in the brightness of active galactic nuclei can be expected [4,5]. The galaxy NGC 4151 (Seyfert 1.5), with coordinates $\alpha(2000) = 12^{\text{h}} 10^{\text{m}} 32.57^{\text{s}}$ and $\delta(2000) = +39^{\circ} 24' 21.06''$, has a redshift of $z = 0.00332$ [6]. The distance to this galaxy has been estimated using two methods. Using the Expanding Photosphere Method, the authors derived $D = (20.0 \pm 1.6)$ Mpc, while the standard candle method gives $D = (16.6 \pm 1.1)$ Mpc. The average distance is therefore $D = (18.3 \pm 1.35)$ Mpc [7]. The mass of its central supermassive black hole (SMBH) is estimated to be $\sim (3-4) \times 10^7 M_{\odot}$ [8].

NGC 4151 is one of the most thoroughly studied Seyfert galaxies, as it exhibits significant variability across all wavelength ranges except the radio band. Measurements have shown that the variability delays of the infrared flux relative to the UV and optical variations are ≈ 37 days, which may be associated with changes in the luminosity of the central energy source [9]. An important feature of NGC 4151 is the variability of the emission-line and continuum fluxes. During a 15 day monitoring campaign in 1993, sharp flux changes with time intervals of up to 70 minutes were detected [10]. Long-term

observations using the reverberation-mapping method (1994—2022) made it possible to identify the connection between the dynamics of the $H\beta$ broad-line region and changes in the luminosity [11]. A component was found in the light curve whose variations occur with a period of about 16 (15.7) years. The authors interpret these cyclic periods as the characteristic dynamical timescale of accretion processes [12].

The aim of this study is to investigate the photometric and spectral characteristics of NGC 4151, including the analysis of brightness variability and emission-line parameters, based on new observations carried out at the Fesenkov Astrophysical Institute (FAI) and the Nasreddin Tusi Shamakhy Astrophysical Observatory (ShAO).

2. Materials and Methods

Photometric observations of the Seyfert galaxy NGC 4151 were carried out at the Tien Shan Astronomical Observatory (TShAO) of the Fesenkov Astrophysical Institute using the Zeiss-1000 "East" telescope ($F = 6600$ mm, $D = 1$ m). The angular field of view of a single CCD frame is $19' \times 19'$. For the observations and image acquisition, several CCD cameras manufactured by Apogee were used: U9000D9 prior to 2016, Alta F16M (4096×4096 , $9\ \mu\text{m}$) until November 2021, and since mid-2022 the U9000D9 CCD camera has been employed, together with BVRc Astrodon filters.

Before 2016, the angular scale of the CCD frames was $0.743''/\text{pixel}$ (for 2×2 binning). After 2016, the scale was $0.56''/\text{pixel}$, and after 2021 it became $0.752''/\text{pixel}$. The photometric data reduction was performed using the MaxIm DL 6 software package [13].

Parallel photometric observations of NGC 4151 in the BV and I_c filters were conducted at the Cassegrain focus of the 60-cm telescope of the Shamakhy Astrophysical Observatory named after N. Tusi (Azerbaijan). The telescope is equipped with a CCD photometer with a thermoelectrically cooled CCD matrix ($FLI\ 4096 \times 4096$). The angular scale for 2×2 binning is $1.98''/\text{pixel}$, and the field of view in the focal plane is $17'$ in diameter. The observational data were reduced using the MaxIm DL 4 software package [13].

Spectroscopic observations of NGC 4151 were carried out at the AZT-8 telescope using a long-slit spectrograph and an SBIG STT-3200 CCD camera, as well as with the Zeiss-1000 "West" telescope (TShAO). Wavelength calibration was performed using comparison lamp spectra of He, Ne, and Ar. Absolute flux calibration relied on spectra of standard stars with known energy distributions. Spectral data reduction was performed using the IRAF (Image Reduction and Analysis Facility) software package developed at the National Optical Astronomy Observatory (NOAO) [14].

3. Results of Photometric Data

Photometric observations of the Seyfert galaxy NGC 4151 were carried out during the period 2016–2025. The galaxy images were measured using the differential photometry method with nearby comparison stars. As standards, we used stars from the works G3 by Lyuty [?] and from Roberts [16],[8] while the G4 stars from Lyuty's list were used as control stars. The root-mean-square (RMS) error of the measurements was calculated for each image and is presented in the tables 1, 2. The results of our photometric observations obtained during 2016–2025 in the B , V , and R_c filters are presented in Table 1, and the B , V , and I_c magnitudes of NGC 4151 obtained in 2020–2023 at the Shamakhy Astrophysical Observatory named after N. Tusi are given in Table 2.

Table 1. Photometric measurements of NGC 4151 in the B, V, and R_c bands obtained in 2016–2025 at the FAI.

Date	JD + 2400000	B $\pm \sigma_B$	V $\pm \sigma_V$	$R_c \pm \sigma_{R_c}$
06.02.2020	58885	12.884 \pm 0.002	12.215 \pm 0.001	11.627 \pm 0.001
08.03.2020	58916	12.852 \pm 0.002	12.213 \pm 0.001	11.632 \pm 0.001
18.04.2020	58957	12.839 \pm 0.001	12.206 \pm 0.001	11.631 \pm 0.001
29.01.2021	59243	12.609 \pm 0.001	12.045 \pm 0.001	11.437 \pm 0.001
18.03.2021	59291	12.619 \pm 0.002	12.056 \pm 0.001	11.447 \pm 0.001
10.04.2021	59314	12.447 \pm 0.001	11.939 \pm 0.001	11.350 \pm 0.001
17.04.2022	59686	12.699 \pm 0.002	12.123 \pm 0.001	11.481 \pm 0.001
19.05.2022	59718	13.134 \pm 0.003	12.398 \pm 0.002	11.762 \pm 0.001
04.06.2022	59734	13.032 \pm 0.002	12.333 \pm 0.001	11.728 \pm 0.001
26.02.2023	60001	12.242 \pm 0.001	11.792 \pm 0.002	11.202 \pm 0.001
28.02.2023	60003	12.264 \pm 0.003	11.808 \pm 0.002	11.200 \pm 0.002
28.02.2023	60003	12.244 \pm 0.001	11.807 \pm 0.002	11.200 \pm 0.001
14.03.2023	60017	12.232 \pm 0.001	11.783 \pm 0.002	11.180 \pm 0.001
24.03.2023	60027	12.243 \pm 0.001	11.724 \pm 0.001	11.151 \pm 0.001
22.04.2023	60056	12.186 \pm 0.002	11.744 \pm 0.001	11.149 \pm 0.001
25.04.2023	60059	12.198 \pm 0.001	11.765 \pm 0.001	11.161 \pm 0.001
04.05.2023	60068	12.319 \pm 0.002	11.848 \pm 0.001	11.219 \pm 0.001
15.05.2023	60079	12.266 \pm 0.001	11.831 \pm 0.001	11.224 \pm 0.001
29.05.2023	60093	12.425 \pm 0.001	11.930 \pm 0.001	11.305 \pm 0.001
30.05.2023	60094	12.396 \pm 0.001	11.913 \pm 0.001	11.293 \pm 0.001
08.06.2023	60103	12.320 \pm 0.001	11.864 \pm 0.001	11.251 \pm 0.001
24.06.2023	60119	12.209 \pm 0.001	11.776 \pm 0.001	11.186 \pm 0.001
02.02.2024	60342	12.027 \pm 0.001	11.636 \pm 0.001	11.046 \pm 0.001
17.03.2024	60386	12.023 \pm 0.001	11.618 \pm 0.001	11.018 \pm 0.001
07.04.2024	60407	12.043 \pm 0.001	11.642 \pm 0.001	11.044 \pm 0.001
14.05.2024	60444	11.989 \pm 0.005	11.594 \pm 0.001	11.014 \pm 0.001
25.01.2025	60700	12.003 \pm 0.001	11.599 \pm 0.001	11.015 \pm 0.001
05.02.2025	60711	11.850 \pm 0.001	11.497 \pm 0.001	10.958 \pm 0.001
04.03.2025	60738	11.981 \pm 0.001	11.587 \pm 0.001	11.011 \pm 0.001
10.03.2025	60744	12.103 \pm 0.001	11.670 \pm 0.001	11.074 \pm 0.001
13.03.2025	60747	12.064 \pm 0.001	11.647 \pm 0.001	11.076 \pm 0.001
31.03.2025	60765	12.154 \pm 0.001	11.729 \pm 0.001	11.140 \pm 0.001
03.04.2025	60768	12.072 \pm 0.001	11.667 \pm 0.001	11.104 \pm 0.001
12.04.2025	60777	11.978 \pm 0.001	11.592 \pm 0.001	11.036 \pm 0.001
25.04.2025	60790	11.859 \pm 0.001	11.519 \pm 0.001	10.985 \pm 0.001
03.05.2025	60798	12.064 \pm 0.001	11.674 \pm 0.001	11.076 \pm 0.001
15.05.2025	60810	11.859 \pm 0.001	11.509 \pm 0.001	10.980 \pm 0.001

Table 2. B , V , and I_c magnitudes of NGC 4151 obtained during 2020–2023 at ShAO.

Date	JD + 2400000	$B \pm \sigma_B$	$V \pm \sigma_V$	$I_c \pm \sigma_{I_c}$
28.01.2020	58877	12.923 ± 0.003	12.211 ± 0.003	11.469 ± 0.004
27.02.2020	58907	12.880 ± 0.003	12.238 ± 0.003	11.463 ± 0.004
18.05.2020	58988	12.815 ± 0.003	12.219 ± 0.003	11.490 ± 0.004
21.05.2020	58991	12.839 ± 0.003	12.202 ± 0.003	11.474 ± 0.004
09.06.2020	59010	13.018 ± 0.003	12.293 ± 0.003	11.574 ± 0.004
14.06.2020	59015	13.069 ± 0.003	12.344 ± 0.003	11.643 ± 0.004
19.07.2020	59050	13.165 ± 0.003	12.436 ± 0.003	11.670 ± 0.004
20.07.2020	59051	13.171 ± 0.003	12.416 ± 0.003	11.660 ± 0.004
11.02.2021	59257	12.630 ± 0.003	12.050 ± 0.003	11.253 ± 0.003
13.04.2021	59318	12.690 ± 0.003	11.920 ± 0.003	11.340 ± 0.003
13.05.2021	59348	12.530 ± 0.003	11.990 ± 0.003	11.235 ± 0.003
14.05.2021	59349	12.880 ± 0.003	11.990 ± 0.003	11.239 ± 0.003
29.05.2021	59364	12.780 ± 0.003	12.170 ± 0.003	11.347 ± 0.003
02.07.2021	59398	12.510 ± 0.003	11.970 ± 0.003	11.246 ± 0.003
05.07.2021	59401	12.550 ± 0.003	11.950 ± 0.003	11.265 ± 0.003
11.07.2021	59407	12.340 ± 0.003	12.030 ± 0.003	11.301 ± 0.003
11.09.2021	59469	12.340 ± 0.003	11.870 ± 0.003	11.172 ± 0.003
07.12.2021	59556	12.330 ± 0.003	11.750 ± 0.003	11.055 ± 0.003
18.07.2022	59779	12.520 ± 0.003	12.190 ± 0.003	11.484 ± 0.004
03.09.2022	59826	12.060 ± 0.003	11.900 ± 0.003	11.259 ± 0.003
29.03.2023	60033	12.040 ± 0.003	11.780 ± 0.003	10.973 ± 0.003

The light curve of NGC 4151 in the B and V filters, constructed from the TShAO data (blue and green squares) and the ShAO data (blue and green crosses), as well as from the additional B -band data of Li et al. (2022) [17] (blue asterisks, JD \approx 57 554–60 033) and the V -band data of Lahue et al. (2025) [18] (green asterisks, JD \approx 60 300–60 600), is shown in Figure 1. The horizontal axis represents the Julian Date (JD–2400000), while the vertical axis shows the apparent magnitude in the B and V filters.

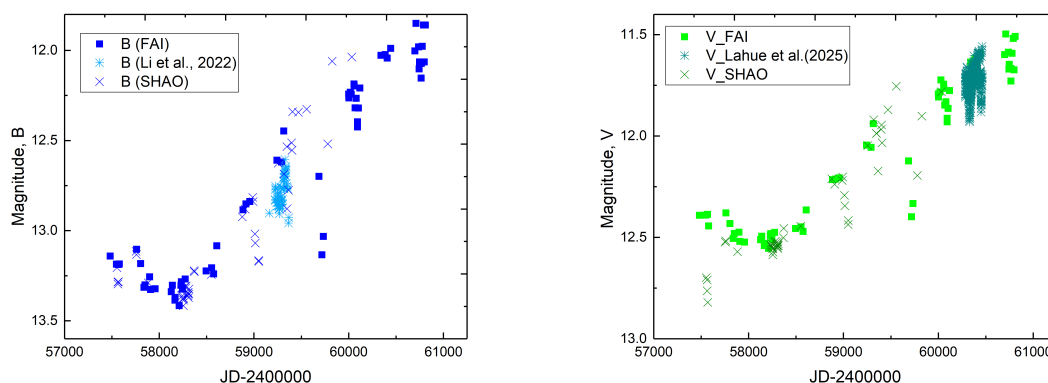


Figure 1. Light curve of NGC 4151 in the B and V filters, constructed from the TShAO data (blue and green squares), ShAO data (blue and green crosses), Li et al. (2022) [17] (blue asterisks), and Lahue et al. (2025) [18] (green asterisks).

The light curve of NGC 4151 in the R_c and I_c filters, constructed from the TShAO data (red squares) and the ShAO data (red asterisks), is shown in Figure 2. The horizontal axis represents the Julian Date (JD–2400000), while the vertical axis shows the apparent magnitude in the R_c and I_c filters.

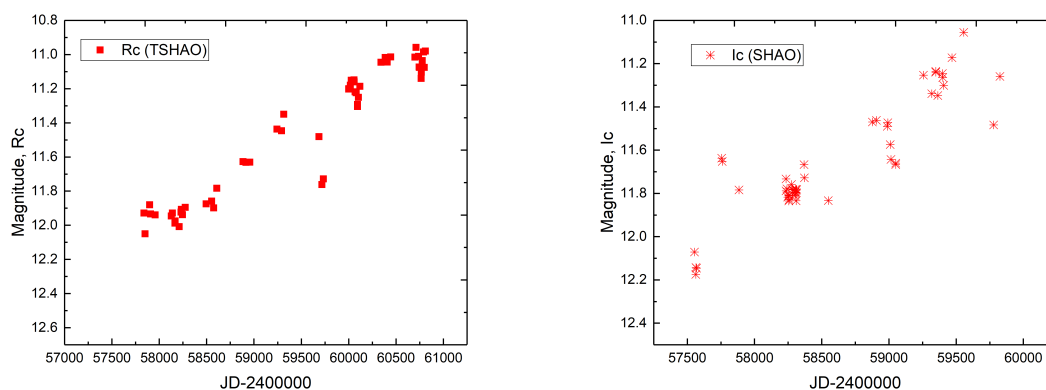


Figure 2. Light curve of NGC 4151 in the R_c and I_c filters constructed from the TShAO observations (red squares) and the ShAO observations (red asterisks).

As seen from the light curves presented in Figures 1 and 2, both an increase and a decrease in the brightness of the galaxy are observed synchronously in all filters. No periodicity in the brightness variations of NGC 4151 was detected during our observing campaign. The largest amplitude changes occurred in the period from 17 April 2022 to 29 March 2023, amounting to $\Delta B = 0.659$, $\Delta V = 0.459$, $\Delta R_c = 0.156$, and $\Delta I_c = 0.245$ magnitudes, respectively. As follows from the light curves and the photometric analysis, the Seyfert galaxy NGC 4151 exhibited significant brightness variations throughout the entire observational period. The FAI data and the measurements reported by Lahue et al. (2025) [18] agree well in the interval $JD \approx 60\,300\text{--}60\,600$, where variability of about 0.3–0.4 mag is observed, confirming the variable nature of this galaxy.

The FAI (TShAO) data, shown in Figure 3, reveal a typical Active Galactic Nuclei (AGN) characteristic: the $(B-V)$ color index increases as the brightness decreases. This trend is explained by the weakening of the blue continuum and the subsequent prominence of the more stable red emission. At the same time, the $(V-R_c)$ index remains nearly constant, indicating a relatively stable contribution of the $H\alpha$ emission. The observed color–magnitude dependence is consistent with previously reported results for NGC 4151 [19,20].

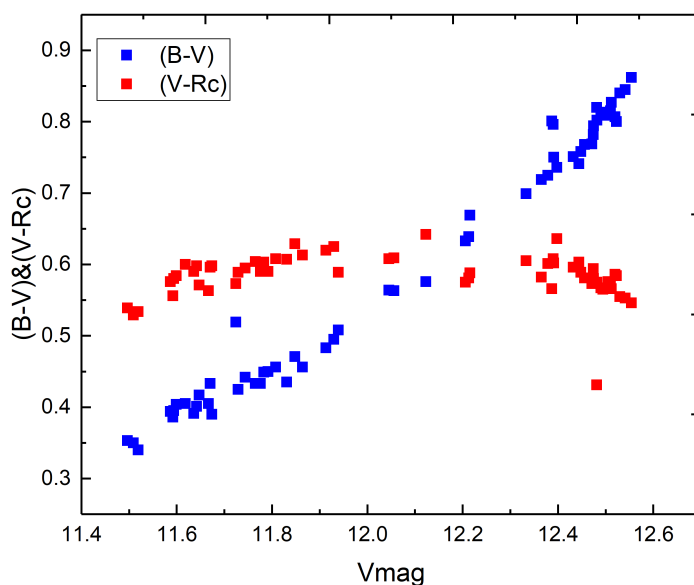


Figure 3. General behavior of the color indices as a function of brightness for the galaxy NGC 4151 (TShAO data).

Figure 4 presents the results of the discrete correlation function (DCF) calculations for the filter pairs B–V and V–R_c for NGC 4151, computed following the method of Edelson & Krolik (1988) [21]. This approach can be used to investigate possible periodicities in the light curves. The x-axis shows the time lag (delay) in years, while the y-axis displays the DCF correlation coefficient. The DCF values represent the mean correlation within each time bin, and the corresponding lags are the central values of these delay intervals. The adopted bin size is 10 days. The number of contributing pairs was determined using the criterion described in Guo et al. [22]:

$$-\Delta\tau/2 < t_{ij} < +\Delta\tau/2.$$

The lag values at which the peaks appear indicate possible periodic components in the light curve. Positive lags imply that variations in the B band occur earlier than those in V. The peak height reflects the strength of the correlation. The plots show a combination of short-, intermediate-, and long-term cycles. The most significant peaks are found in the range from 0.5 to 3.5 years. A clear and strongest peak is observed at a lag of 0.56 years in both B–V and V–R_c, though with different amplitudes. This peak represents genuine physical variability of the source—corresponding to a stable and global process in the accretion disk—rather than random fluctuations. The difference in peak strength indicates that the variability is chromatic.

Several non-exact harmonics of the main peak are also present at lags of approximately 1.25, 1.9, 2.5, 3.35, and 4.3 years. In addition, the presence of negative peaks further supports the interpretation that the observed variability is chromatic in nature.

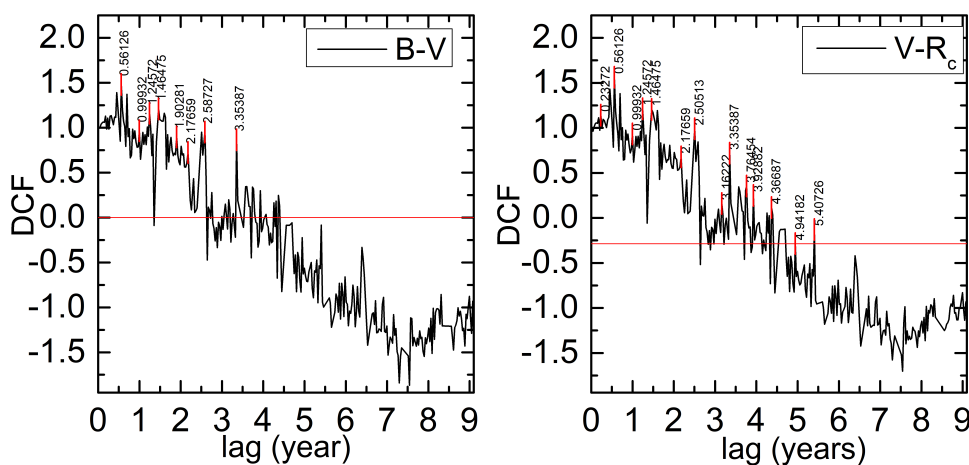


Figure 4. Results of the discrete correlation function for NGC 4151 (TShAO data)

3.1. Results of Spectral Observations of NGC 4151

The brightness of the galaxy NGC 4151 and its spectral characteristics can vary significantly over time. These variations also affect the emission lines, including the Balmer lines ($H\alpha$, $H\beta$, etc.). The Balmer lines, especially $H\alpha$ and $H\beta$, are among the dominant features in the spectrum of NGC 4151 and contain important information about the physical conditions and kinematics of the gas in the active galactic nucleus. The profiles of the Balmer lines in NGC 4151 exhibit a complex structure and may change with time. Such variations indicate changes in the distribution and motion of the gas responsible for the emission.

The Table 3 below presents the measured fluxes in the continuum and in the emission lines, as well as several characteristics of the emission-line profiles. It should be noted that in the red spectral region, the reported values correspond to the total fluxes of the $H\alpha + [N\text{II}] \lambda\lambda 6548, 6583 \text{ \AA}$ and $[S\text{II}] \lambda\lambda 6717, 6731 \text{ \AA}$ emission lines.

Table 3. Spectral line parameters and continuum/line fluxes of NGC 4151.

Date	λ (Å)	Continuum Flux ($\text{erg s}^{-1} \text{cm}^{-2} \text{Å}^{-1}$)	Line Flux ($\text{erg s}^{-1} \text{cm}^{-2}$)	EW (Å)	FWHM (Å)	Telescope
17.04.2020	4859.336	8.378E-14	2.902E-12	35	22	West 1 m, TShAO
	4960.098	8.417E-14	5.620E-12	66	8	
	5007.523	8.840E-14	1.825E-11	206	8	
23.04.2021	6302.772	5.390E-14	7.652E-13	14	13	AZT-8
	6564.355	5.683E-14	2.431E-11	428	63	
	6724.901	4.930E-14	1.749E-12	35	23	
31.03.2022	6300.296	4.744E-14	7.732E-13	16	10	AZT-8
	6364.729	4.792E-14	3.344E-13	7	14	
	6562.976	5.000E-14	2.611E-11	522	67	
	6724.010	4.567E-14	1.849E-12	40	25	
28.02.2023	6299.590	3.651E-14	5.309E-13	15	11	AZT-8
	6560.780	3.862E-14	1.599E-11	414	65	
	6723.590	3.336E-14	1.061E-12	32	27	
25.03.2023	4862.556	2.318E-13	1.624E-11	70	63	AZT-8
	4961.336	2.596E-13	6.023E-12	23	13	
	5008.703	2.581E-13	1.096E-11	42	17	
12.04.2023	6302.412	5.540E-14	6.842E-13	12	11	AZT-8
	6367.008	5.740E-14	3.426E-13	6	15	
	6564.198	6.774E-14	2.669E-11	394	67	
	6725.933	6.309E-14	1.576E-12	25	26	
27.04.2023	6303.415	5.506E-14	6.458E-13	12	11	AZT-8
	6368.211	5.518E-14	2.445E-13	4	12	
	6564.869	6.051E-14	2.638E-11	436	67	
	6726.645	5.049E-14	1.699E-12	34	25	
29.05.2023	4857.798	6.990E-14	6.354E-12	91	58	AZT-8
	4958.809	7.283E-14	4.135E-12	57	10	
	5006.948	6.900E-14	1.290E-11	187	10	
18.03.2024	6300.789	6.240E-14	5.612E-13	9	9	AZT-8
	6364.924	6.183E-14	2.824E-13	5	14	
	6563.661	6.452E-14	2.752E-11	427	70	
	6725.709	5.901E-14	1.545E-12	26	24	
07.04.2024	6300.177	7.194E-14	6.903E-13	10	11	AZT-8
	6364.516	7.425E-14	3.050E-13	4	68	
	6563.539	7.771E-14	2.852E-11	367	26	
	6724.437	6.514E-14	1.736E-12	27	–	
07.05.2024	4862.180	8.208E-14	7.216E-12	88	66	AZT-8
	4961.292	8.884E-14	3.364E-12	39	9	
	5009.577	8.433E-14	1.106E-11	131	9	
	6304.229	6.848E-14	7.414E-13	11	12	
	6369.560	7.355E-14	3.956E-13	5	16	
	6568.734	7.823E-14	3.135E-11	400	69	
	6728.888	6.885E-14	1.855E-12	27	25	
27.05.2024	6300.002	6.650E-14	8.722E-13	13	16	AZT-8
	6366.348	7.188E-14	3.236E-13	5	23	
	6564.075	7.250E-14	2.689E-11	371	68	
	6723.241	6.642E-14	1.468E-12	22	27	

Figure 5 shows the spectral energy distribution (SED) of NGC 4151 constructed from the data in Table 3. The X-axis represents the wavelength, while the Y-axis shows $\log(\lambda F(\lambda))$. The resulting SED illustrates the continuum levels at different wavelengths during the observation periods and allows us to assess their variability over time.

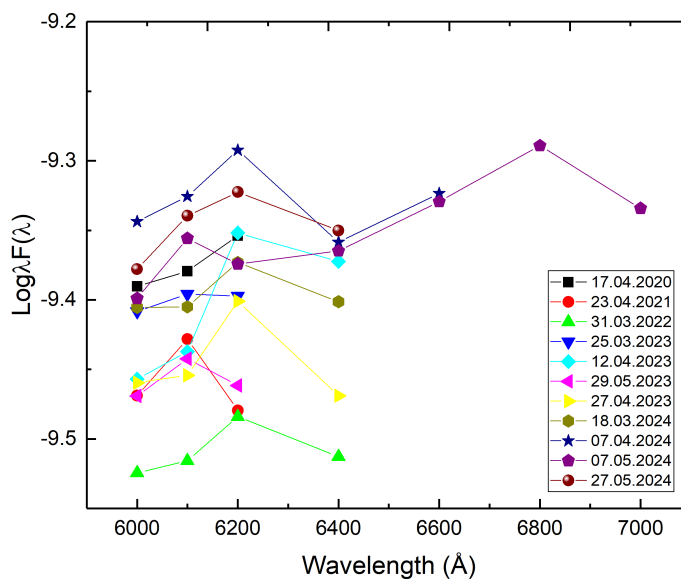


Figure 5. Spectral energy distribution (SED) of NGC 4151. The X-axis represents wavelength, and the Y-axis represents $\log(\lambda F(\lambda))$.

To obtain a quantitative estimate of the size of the broad-line region (BLR) at different epochs, we calculated the continuum luminosity at $\lambda 5100 \text{ \AA}$ (L_{5100}) using the luminosity distance to NGC 4151 of $D_L = 19 \text{ Mpc}$, as determined by Sebastian et al. (2014) [?], and applied the empirical R - L relation [19] derived in that study. The results are summarized in Table 4. The characteristic BLR size varies from approximately 0.13 to 0.15 light days over the different observing epochs.

Table 4. Flux, luminosity, and BLR size estimates for NGC 4151.

Epoch (Date)	$F_{5100} \text{ (erg cm}^{-2} \text{ s}^{-1} \text{ \AA}^{-1}\text{)}$	$L_{5100} \text{ (erg s}^{-1}\text{)}$	$R_{\text{BLR}} \text{ (light-days)}$
17.04.2020	8.84×10^{-14}	3.82×10^{39}	0.15
25.03.2023	8.00×10^{-14}	3.47×10^{39}	0.14
29.05.2023	6.90×10^{-14}	2.98×10^{39}	0.13
07.05.2024	8.43×10^{-14}	3.64×10^{39}	0.14

4. Discussion

We carried out photometric and spectroscopic observations of the Seyfert galaxy NGC 4151 in the optical range in order to investigate its variability. The photometric light curves obtained in four filters (B , V , R_c , I_c) show similar behavior (Figures 1 and 2), and the photometric uncertainties do not exceed 0.001–0.004 mag, confirming the high quality of the observational material. Over the entire monitoring interval, the variability amplitude reaches ~ 0.9 – 1.0 mag, which is consistent with the well-known high activity level of this Seyfert nucleus.

Comparison of our measurements with previously published data shows good agreement. The fluxes in the B filter obtained at FAI, SHAO, and in Li et al. [?] agree well over the interval JD 57554–60033. The V -band data from FAI and Lahue et al. [?] also coincide in the range JD $\approx 60\,300$ – $60\,600$, where variability of about 0.3–0.4 mag is observed. This confirms the reliability of our photometric series. No stable periodicities were detected in the brightness variations of NGC 4151. The largest brightness changes occurred between 17 April 2022 and 29 March 2023: $\Delta B = 0.659$, $\Delta V = 0.459$, $\Delta R_c = 0.156$, and $\Delta I_c = 0.245$ mag.

Analysis of the color indices ($B - V$) and ($V - R_c$) obtained at TShAO shows that the object exhibits a complex structure typical of AGN. A clear “bluer-when-brighter” trend is observed, where

NGC 4151 becomes noticeably bluer as it brightens. This behavior is consistent with variations of the accretion-disk continuum, which strengthens as the ionizing activity of the nucleus increases.

The discrete correlation function (DCF) analysis revealed significant correlation peaks in the lag range 0.5–3.5 years. Peaks detected simultaneously in the $B - V$ and $V - R_c$ dependencies (Figure 3) indicate the presence of quasi-periodic components in the light curve. Positive lags imply that variations in the B band precede those in V, which is consistent with a scenario in which disturbances propagate from the hotter inner regions of the accretion disk to the cooler outer zones. The strongest peak at a lag of ≈ 0.56 years may represent a characteristic delay time between disk regions or the dynamical timescale of structural readjustment within the accretion flow.

The spectroscopic data further confirm the variability of NGC 4151. Both the brightness and the spectral properties change significantly over time, including variations in the profiles of the dominant Balmer lines ($H\alpha$, $H\beta$). Changes in their shape and intensity reflect modifications in the distribution and kinematics of the gas in the broad-line region (BLR). The spectral energy distribution (SED) shows that the lowest $\log \lambda F(\lambda)$ values occur on 31 March 2022 and 18 March 2024, indicating states of reduced AGN activity. In contrast, the highest continuum levels, recorded on 7 April 2024, 7 May 2024, and 27 May 2024, correspond to phases of increased activity, where the continuum strengthens and the SED slope becomes flatter. This behavior is consistent with enhanced thermal emission from the accretion disk and an increase in ionizing flux.

The characteristic BLR size varies between 0.13 and 0.15 light days at different epochs, which is consistent with previous estimates for NGC 4151 and indicates a relatively compact broad-line region. The combined photometric, spectroscopic, and correlation results show that the variability of NGC 4151 is driven by complex internal processes within the accretion disk and BLR, including structural changes in the disk geometry, variations in the accretion rate, and the response of the emitting gas to fluctuations in the ionizing radiation.

5. Conclusions

This study details the findings from ongoing photometric and spectroscopic monitoring of the Seyfert galaxy NGC 4151. The photometric data were acquired at two facilities: the Fesenkov Astrophysical Institute (Almaty, Kazakhstan) and the Nasreddin Tusi Shamakhi Astrophysical Observatory (Shamakhi, Azerbaijan), while the spectroscopic observations were conducted solely at FAI.

The B , V , R_c , and I_c light curves exhibit a consistent structure (Figures 1 and 2), with the most significant brightness variability observed between 17 April 2022 and 29 March 2023, registering amplitudes of $\Delta B = 0.659$, $\Delta V = 0.459$, $\Delta R_c = 0.156$, and $\Delta I_c = 0.245$ mag. Analysis via the discrete correlation function (DCF) identified a prominent peak at a time lag of approximately 0.56 years. This feature is hypothesized to represent either the characteristic timescale for perturbation propagation within the accretion disk or the dynamical timescale associated with structural reconfiguration of the disk.

The spectral energy distribution (SED) analysis indicates that the lowest $\log \lambda F(\lambda)$ values were measured on 31 March 2022 and 18 March 2024, corresponding to intervals of diminished AGN activity (Figure 5). Conversely, the data collected on 7 April 2024, 7 May 2024, and 27 May 2024 reflect phases of heightened activity, characterized by a stronger continuum and a flatter SED slope.

The characteristic size of the broad-line region (BLR) was found to vary between 0.13 and 0.15 light days across different epochs, a result which is in good agreement with prior estimates for NGC 4151.

These findings underscore the intricate and multi-component nature of the physical processes operative in the central engine of NGC 4151. Continued high-cadence monitoring, coupled with detailed decomposition of emission-line profiles into constituent components and the determination of the physical parameters of the emitting regions, is essential for advancing our understanding of the accretion disk structure and the kinematics of the BLR.

Author Contributions: Conceptualization, methodology and visualization, N.H., S.S. and A.S.; formal analysis, A.S.; validation, S.R. and G.N.; formal analysis, L.K.; investigation, S.S. and L.K.; resources, I.V., N.H. and S.R.;

data curation, G.N, S.S. and L.A.; writing—original draft preparation, review and editing, N.H., S.S., A.S., L.K. and G.N; supervision, project administration and funding acquisition, S.S. All authors have read and agreed to the published version of the manuscript.

Funding: This research is funded by the Ministry of Science and Higher Education of the Republic of Kazakhstan (Grant No. BR24992607).

Acknowledgments: The authors express their gratitude to the SHAO team and the FAI observers for their assistance in organizing and conducting the spectral and photometric observations.

Conflicts of Interest: The authors declare no conflicts of interest. The funders had no role in the design of the study, in the collection, analyses or interpretation of data, in the writing of the manuscript or in the decision to publish the results.

References

- Antonucci, R. *Unified Models for Active Galactic Nuclei and Quasars*. **Annual Review of Astronomy and Astrophysics** **1993**, *31*, 473–521. doi:10.1146/annurev.aa.31.090193.002353.
- Merkulova, N.I. *UBVRI Light Curves of the Seyfert Galaxy NGC 7469 During 1990–1998: Microvariability*. **Astronomical Journal** **2000**, *119*, 631. doi:10.1086/301199.
- Denissyuk, E.K.; Valiullin, R.R.; Shomosheikova, S.A.; Kondratyeva, L.N.; Reva, I.V.; Aimanova, G.A.; Krugov, M.A. *Results of Spectral Observations of 15 Seyfert Galaxies*. **Astrophysics** **2022**, *65*, 447–455. doi:10.1007/s10511-023-09753-7.
- Grafton-Waters, S.; Branduardi-Raymont, G.; Mehdipour, M.; Page, M.J.; Behar, E.; Kaastra, J.; Arav, N.; Bianchi, S.; Costantini, E.; Ebrero, J.; et al. *Multi-wavelength campaign on NGC 7469. VI. Photoionisation modelling of the emission line regions and the warm absorber*. **A&A** **2020**, *633*, A62. arXiv:1907.01946. doi:10.1051/0004-6361/201935815.
- Nandi, P.; Chakrabarti, S.K.; Mondal, S. *Spectral Properties of NGC 4151 and the Estimation of Black Hole Mass Using TCAF Solution*. **ApJ** **2019**, *877*, 65. arXiv:1905.02147. doi:10.3847/1538-4357/ab1d62.
- Hönig, S.F.; Watson, D.; Kishimoto, M.; Hjorth, J. *A dust-parallax distance of 19 megaparsecs to the supermassive black hole in NGC 4151*. **Nature** **2014**, *515*, 528–530. doi:10.1038/nature13914.
- Tsvetkov, D.Y.; Baklanov, P.V.; Potashov, M.S.; Oknyansky, V.L.; Mikailov, K.M.; Huseynov, N.A.; Alekberov, I.A.; Khalilov, O.V.; Pavlyuk, N.N.; Metlov, V.G.; et al. *Supernova 2018aoq and a distance to Seyfert galaxy NGC 4151*. **MNRAS** **2019**, *487*, 3001–3006. arXiv:1904.06586. doi:10.1093/mnras/stz1474.
- Roberts, C.A.; Bentz, M.C.; Vasiliev, E.; Valluri, M.; Onken, C.A. *The Black Hole Mass of NGC 4151 from Stellar Dynamical Modeling*. **ApJ** **2021**, *916*, 25. doi:10.3847/1538-4357/ac082d.
- Oknyansky, V.L.; Shenavrin, V.I.; Metlova, N.V.; Gaskell, C.M. *The Relative Wavelength Independence of IR Time Lags in NGC 4151 During 2010–2015*. **Astronomy Letters** **2019**, *45*, 197–207.
- Vedavathi, P.; Doddamani, V.H. *Short timescale UV variability study in NGC 4151 using IUE data*. **JAA** **2018**, *39*, 55. doi:10.1007/s12036-018-9539-0.
- Chen, Y.J.; Bao, D.W.; Zhai, S.; Fang, F.N.; Hu, C.; Du, P.; Yang, S.; Yao, Z.H.; Li, Y.R.; Brotherton, M.S.; et al. *Broad-line region in NGC 4151 monitored by two decades of reverberation mapping campaigns – I. Evolution of structure and kinematics*. **MNRAS** **2023**, *520*, 1807–1831. doi:10.1093/mnras/stad051.
- Oknyanskij, V.L.; Metlova, N.V.; Huseynov, N.A.; Guo, D.F.; Lyuty, V.M. *Optical Monitoring of NGC4151 During 110 Years*. **Odessa Astronomical Publications** **2016**, *29*, 95. doi:10.18524/1810-4215.2016.29.85058.
- Astronomical Imaging Software.
- Fitzpatrick, M.; Placco, V.; Bolton, A.; Merino, B.; Ridgway, S.; Stanghellini, L. *Modernizing IRAF to Support Gemini Data Reduction*. arXiv:2401.01982. doi:10.48550/arXiv.2401.01982.
- Lyuty, V.M. *Optical Variability of the Nuclei of Seyfert Galaxies*. **Soviet Astronomy** **1973**, *16*, 763.
- Roberts, C.A.; Rumstay, K.R. *A Ten-Year Photometric Study of Selected Active Galaxies*. **JSARA** **2012**, *6*, 47–58.
- Li, S.S.; Feng, H.C.; Liu, H.T.; Bai, J.M.; Li, R.; Lu, K.X.; Wang, J.G.; Huang, Y.K.; Zhang, Z.X. *Velocity-resolved Reverberation Mapping of Changing-look AGN NGC 4151 during Outburst Stage*. **ApJ** **2022**, *936*, 75. doi:10.3847/1538-4357/ac8745.
- Lahue, V.; Bentz, M.C.; Padrick, N. *The V-band Variability of NGC 4151*. **RNAAS** **2025**, *9*, 48. doi:10.3847/2515-5172/adbbf0.
- Bentz, M.C.; Denney, K.D.; Grier, C.J.; et al. *The Low-luminosity End of the Radius–Luminosity Relationship for AGN*. **ApJ** **2013**, *767*, 149. doi:10.1088/0004-637X/767/2/149.

20. Merkulova, N.I.; Doroshenko, V.T.; Lyuty, V.M.; et al. *Characteristics of the continuum variability of the nucleus of NGC 4151*. **A&A** **2001**, *371*, 771–782. doi:10.1051/0004-6361:20010304.
21. Edelson, R.A.; Krolik, J.H. *The Discrete Correlation Function: a new method for analyzing unevenly sampled variability data*. **ApJ** **1988**, *333*, 646–659. doi:10.1086/166773.
22. Guo, D.F.; Hu, S.M.; Chen, X.; Gao, D.W.; Qu, J.L. *Optical monitoring of the Seyfert galaxy NGC 4151 and possible periodicities in its historical light curve*. **RAA** **2014**, *14*, 923–938. doi:10.1088/1674-4527/14/8/007.

Disclaimer/Publisher's Note: The statements, opinions and data contained in all publications are solely those of the individual author(s) and contributor(s) and not of MDPI and/or the editor(s). MDPI and/or the editor(s) disclaim responsibility for any injury to people or property resulting from any ideas, methods, instructions or products referred to in the content.